Monitoring of Skeletal Progression of Prostate Cancer by GFP Imaging, X-Ray, and Serum OPG and PTHrP

D.W. Burton,[1] J. Geller,[2] M. Yang,[2] P. Jiang,[2] I. Barken,[3] R.H. Hastings,[4] R.M. Hoffman,[2,5] and L.J. Deftos[1]*

[1]*Department of Medicine, University of California and San Diego Veterans Administration Healthcare System (VASDHS), San Diego, California*

[2]*AntiCancer, Inc., San Diego, California*

[3]*Prostate Cancer Research and Education Foundation (PCREF), San Diego, California*

[4]*Department of Anesthesiology, University of California and San Diego Veterans Administration Healthcare System (VASDHS), San Diego, California*

[5]*Department of Surgery, University of California, San Diego, California*

BACKGROUND. Prostate cancers (PCas) produce factors that can serve as biomarkers for tumor metastasis and bone progression. Transduced GFP expression by cancer cells can be imaged to monitor therapy. We exploited both concepts by developing a GFP-expressing PCa cell line that expresses PTHrP and studying it in an animal model of malignancy with methods that assess the skeletal progression of this tumor.

METHODS. We developed a GFP-producing PCa cell line by stable transduction of PC-3 PCa cells. This PC-3 variant was used to study tumor progression in an immunocompromised mouse model. Skeletal progression of the PCa cells and the effects of pamidronate administration were evaluated radiologically, fluorometrically, and by measurement of serum tumor markers.

RESULTS. The PC-3 cells produced extensive bone lesions when injected into the tibia of immunocompromised mice. The skeletal progression of the PC-3 cells could be monitored by GFP optical imaging, X-ray, and by measurements of tumor products in serum, notably PTHrP and OPG. Pamidronate treatment reduced tumor burden as assessed at autopsy by imaging and biomarkers.

CONCLUSIONS. Pamidronate treatment exhibited anti-tumor effects that were reflected by decreases in serum PTHrP, OPG, and by GFP and radiological imaging procedures. Imaging of GFP expression enables real-time monitoring of tumor growth in the bone. PTHrP and OPG may be useful as tumor biomarkers for PCa that has metastasized to bone. This novel human PCa model can be used to study the clinical potential of diagnostic and therapeutic modalities in the skeletal progression of PCas. *Prostate 62: 275–281, 2005.* © 2004 Wiley-Liss, Inc.

KEY WORDS: **tumor markers; metastases; bisphosphonates; green fluorescent protein; immunoassay**

Abbreviations: PCa, prostate cancer; GFP, green fluorescent protein; PBS, phosphate buffered saline; SEM, standard error of the mean; PTHrP, parathyroid hormone-related protein; RANK, receptor activator of NF-kappa B; RANKL, receptor activator of NF-kappa B ligand; OPG, osteoprotegrin; i.v., intravenous; IL, interleukin.

Grant sponsor: VA Merit Review Grants; Grant sponsor: PCREF; Grant sponsor: NIH; Grant numbers: DK-60586, AR47347, ES-09227; Grant sponsor: DOD Prostate Cancer Research Program Award; Grant number: DAMD17-01-1-0016.

*Correspondence to: L.J. Deftos, MD, Department of Medicine (111-C), University of California and San Diego Veterans Administration Healthcare System (VASDHS), 3350 La Jolla Village Dr., San Diego, California 92161. E-mail: ljdeftos@ucsd.edu.

Received 19 April 2004; Accepted 9 June 2004
DOI 10.1002/pros.20146
Published online 23 July 2004 in Wiley InterScience (www.interscience.wiley.com).

INTRODUCTION

Prostate cancer (PCa) is the most prevalent cancer in adult males; and despite increasing efforts at early detection, 10–20% of the patients will demonstrate metastases at the time of diagnosis [1,2]. Bone is a common site of PCa metastases, and bone metastases are responsible for most of the morbidity associated with this disease, such as bone pain and fractures [1,2]. The tendency of PCa to spread to the skeleton indicates that tumor products favor growth in bone. PCa cells express many factors that regulate osteoblasts and osteoclasts, including parathyroid hormone-related protein (PTHrP) [3], receptor activator of NF-kappa B (RANK), receptor activator of NF-kappa B ligand (RANKL), and osteoprotogerin (OPG) [4,5]. The effects of these factors may explain, in part, the ability of PCa cells to interact with the bone environment.

RANKL (also known as OPGL, ODF, and TRANCE), a cell membrane bound member of the tumor necrosis family superfamily, stimulates osteoclast differentiation and activity by binding to the RANK, which is expressed on the osteoclast precursor cell. OPG is a recently identified participant in skeletal metabolism that interacts with RANK and RANKL [6,7]. OPG serves as a decoy receptor for RANK and inhibits osteoclastogenesis by binding to RANKL, preventing it from binding to RANK.

Substantial in vitro and recent in vivo data show that PTHrP expression regulates the progression of the tumor, especially to bone [8,9]. Because of their effects on osteoclasts, RANK and PTHrP expression could contribute to skeletal metastasis and/or bone growth of PCa. OPG, on the other hand, serves as a decoy receptor to RANK and inhibits osteoclastogenesis by binding to RANKL, preventing it from binding to RANK [6,7]. Consequently, OPG could retard skeletal progression of PCa.

Because these factors are commonly expressed by PCa as well as bone cells [5], they may also be valuable as biomarkers for bone metabolic changes in PCas that have metastasized to the skeleton. Other proteins of interest include the cytokines, interleukin (IL)-6, and IL-8, which are involved in the growth and angiogenic properties of many types of malignancies and can also serve as biomarkers for PCa [10–12]. Biomarkers that also regulate bone metastasis can correlate with bone tumor burden and change in response to therapy.

We investigated several prostate carcinoma-derived proteins with effects in bone as potential markers of skeletal progression in a murine model of prostate carcinoma. This study evaluated the effects of treatment with the bisphosphonate, pamidronate, in immunocompromised mice bearing tibial prostate carcinoma cell xenografts on skeletal progression and levels of calcium, PTHrP, OPG, sRANKL, IL-6, and IL-8. Administration of bisphosphonates is useful in treating prostate, breast, and lung cancer that metastasize to the skeleton [13–17]. They induce apoptosis [18], reduce cell adhesion [19], inhibit angiogenesis [20], and decrease cell proliferation in several PCa cell lines [21,22].

The growth of PCa cells in the bone was monitored by whole-body imaging of green fluorescent protein (GFP) expression in the PCa cells [28].

MATERIALS AND METHODS

Cells

The PC-3 cell line, which was originally isolated from a prostate adenocarcinoma that had metastasized to the bone [23], was used for our studies. These cells metastasize to bone in PCa animal models and produce PTHrP [24–26]. The cells were genetically engineered to express GFP [28] in order to enable convenient visualization and quantitation of the tumor mass. The PC-3-GFP human prostate cells were grown in monolayer in RPMI 1640 media supplemented with 5% fetal bovine serum and incubated in a humidified chamber at 37°C with 95% air and 5% CO_2.

Animals

Six-month-old male, severe combined immunodeficiency (SCID) mice were housed in a barrier filter room and fed Purina rodent chow ad lib. Animal experiments were performed in accordance with the Guidelines for the Care and Use of Laboratory Animals (NIH Publication Number 85-23) under assurance number A3873-01.

Tumor Implantantion and Experimental Course

Subconfluent PC-3-GFP cells were freshly trypsinized, counted, and placed on ice immediately before injection. The mice were injected with 10^6 cells in 15 µl sterile PBS into the bone marrow of the right tibia using a 28-gauge needle and a Hamilton glass syringe. The left tibia served as the negative control. Two months after implantation, the mice were anesthetized, exanguinated for blood collection, and sacrificed. Serum was prepared from blood and transferred to clean microcentrifuge tubes and frozen for subsequent measurements of calcium, PTHrP, OPG, sRANKL, IL-6, and IL-8. Mice were evaluated for tumor growth by GFP expression and X-ray to assess the formation of bone lesions and tumor mass.

Treatment

Pamidronate disodium (Ben Venue Labs, Bedford, OH) or vehicle (PBS) were injected (i.v.) into the tail

vein beginning 1 month prior to intra-tibial implantation of PCa cells. Additional treatments were administered at the time of tumor implantation and at monthly intervals thereafter. Animals were divided into control, low dose, or high dose pamidronate groups (15 mice/group) receiving PBS only (control), 2.2 mg pamidronate/kg body weight (low dose), or 14.4 pamidronate/kg body weight (high dose) i.v. in a volume of 25 μl PBS. The mice tolerated the treatments without any observed adverse side effects.

Fluorescent Imaging

High-magnification imaging of GFP expressing tumors were visualized using a Leica fluorescent stereomicroscope, model LZ12, equipped with a 50 W mercury lamp. Whole-body imaging was carried out in a light box illuminated by blue-light fiber optics (Lightools Research, Encinitas, CA) and imaged using a thermoelectrically cooled color CCD camera [28].

Image Analyses

Fluorescent images were analyzed on a Dell computer equipped with a Pentium 4 processor, 512 MB RAM, and Windows XP Pro operating system (Microsoft Corporation, Redmond, WA) using Image-Pro Plus 4.5.1 software (Media Cybernetics, Silver Spring, MD). The maximum and total green pixel intensity values were quantitated from the digitized images and the data were exported to Microsoft Excel 2000 (Microsoft Corporation) and the results tabulated.

Radiographic Analyses

Skeletal radiographs were exposed with 40 keV for 20 sec in an HP Faxitron 5000 series X-ray cabinet. The Kodak X-Omat TL films were processed in a Kodak film processor. The radiographic images of the mouse tibiae injected with PC-3 cells were quantitated visually using a 10 X De-luxe loop objective by two observers. The semiquantitation scoring method was formulated as 0 = no lesions, 1 = minor changes, 2 = small lesions, 3 = significant lesions (minor peripheral margin breaks, 1–10% of bone surface disrupted), 4 = significant lesions (major peripheral margin breaks. >10% of bone surface disrupted).

Calcium Measurement

Serum calcium was determined by the reaction of calcium with o-cresolphthalein to produce a red complex at pH 10 (Sigma Chemical, St. Louis, MO). The plates were scanned in a plate reader at a wavelength of 570 nm. A reference standard curve was generated to convert the sample optical density values into calcium concentrations.

PTHrP, OPG, IL-6, IL-8, and sRANKL Immunoassays

To evaluate PTHrP, OPG, IL-6, IL-8, and sRANKL utility as biomarkers for tumor mass, the sera from the mice were measured for PTHrP, OPG, and sRANKL levels using immunoassays. The conditioned media and mouse sera were measured for PTHrP by radioimmunoassay [13]. In brief, human PTHrP 38–64 peptide was used as standard and PTHrP 1–86 peptide was radioiodinated by the chloramine T method. Rabbit antiserum to PTHrP 38–64 was used in 3-day non-equilibrium immunoassay format. All samples were assayed in multiple dilutions that paralleled the corresponding PTHrP standard curve. The intra- and inter-assay variations were approximately 7–12%, and the limits of assay sensitivity were 4 pmol/L. The OPG and cytokine (IL-6 and IL-8) immunoassays used antibodies purchased from R and D Systems (Minneapolis, MN) and BioSource International (Camarillo, CA), respectively. These two-site immunoassays were detected with a streptavidin labeled β-D-galactosidase enzyme reaction using the fluorescent substrate, 4-methylumbelliferyl-β-D-galactopyranoside (Calbiochem, San Diego, CA) and had assay sensitivities of 9, 3, and 4 pg/ml, respectively. The human OPG immunoassay kit (DY805) does not cross-react with mouse OPG (R and D Systems). The sRANKL levels were measured using a commercial kit (American Laboratory Products Co., Windham, NH). The reported sensitivity of the sRANKL assay is 0.5 pmol/L.

Statistics

Statistical analyses were performed using Microsoft Excel (Microsoft Corp) and Statview (SAS, Cary, NC) software. Differences among treatment groups were assessed using ANOVAs and two-tailed Student's t tests. Correlation coefficient significance was determined using Documenta Geigy Scientific Tables, 6th Edition. The X-ray scoring differences were tested using Kruskall Wallis ANOVA and the Dunn test for post hoc analyses [29]. A $P \leq 0.05$ was considered to be statistically significant. The data are reported as mean ± standard error of the mean (SEM).

RESULTS

Fluorescent images of the PC-3-GFP injected mice showed large tumors, >1 cm^3, in the majority of the mice (control = 14/15, low dose pamidronate = 11/15, and high dose pamidronate = 8/15 mice). Imaging took place 8 weeks after implantation. X-ray also demonstrated severe osteolytic lesions in the majority of the mice, although some animals in each treatment group had no apparent bone abnormality (control = 1, low dose = 1, and high dose = 3 mice). No radiographic

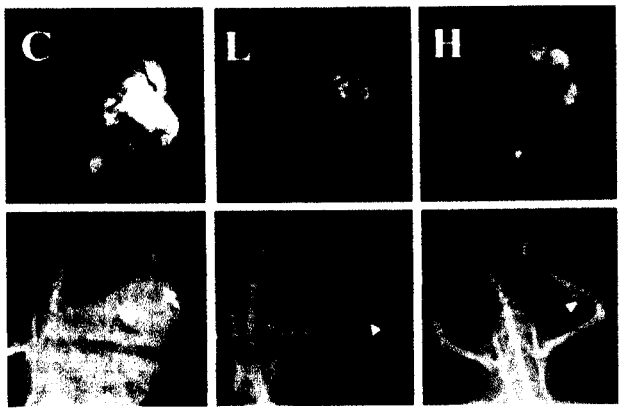

Fig. 1. Representative fluorescent (**top**) and radiographic (**bottom**) images of mice injected with PC-3-GFP cells and treated with vehicle control or pamidronate. Typical images from the three groups are shown, C (vehicle control treated), L (low dose pamidronate), and H (high dose pamidronate). Note the significant decrease in the GFP fluorescent intensity and severity of the bone legions in the pamidronate treatment groups compared to the control treatment group. [Color figure can be viewed in the online issue, which is available at www.interscience.wiley.com.]

abnormalities were observed for the control tibiae or other areas of the skeleton. Examples of the typical fluorescent images and radiographs of the mice skeletons from the three groups are shown in Figure 1.

The mice that were treated with pamidronate demonstrated a slight reduction in the GFP positive area compared to the control treated mice (Fig. 2A). The fluorescent images of the mice were further quantitated for quantitation of the maximum green pixel density values in the tumor area (Fig. 2B). The maximum green fluorescence was centered in the bone tumor rather than extraosseous tumor. Maximum green fluorescent pixel values were significantly reduced in the high dose pamidronate treatment group compared to the control group ($P < 0.05$).

The radiographic severities of the bone lesions were quantitated radiographically as shown in Figure 3. The mice that were treated with a high dose of pamidronate demonstrated a significant reduction ($P < 0.05$) in the severity of the bone lesions compared to the control treated mice. The low-dose pamidronate-treated group showed a reduction in radiographic and GFP scores compared to control treated mice, but they were not significant. The GFP and X-ray score results from the fluorescence and radiographically imaged skeletons were significantly correlated ($r = 0.783$, $P < 0.01$). The density of the maximum green fluorescent pixel, as determined by image analysis, correlated with both the GFP and X-ray scores ($r = 0.594$, $P < 0.01$ and $r = 0.750$, $P < 0.01$, respectively).

The serum calcium levels from the PC-3-GFP tumor-bearing mice were elevated compared to non-tumor

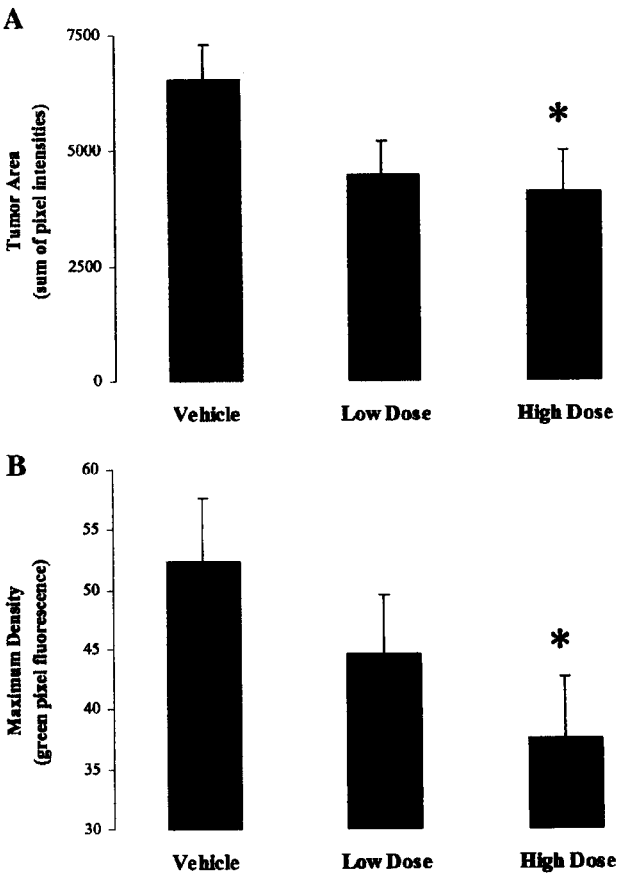

Fig. 2. GFP fluorescence demonstrates that pamidronate reduced the size of the tumor mass by measuring maximum density of the green pixels in the bone tumors. **Panel A**: Scoring results of the fluorescent images of the mouse tibias injected with PC-3-GFP cells. The tumor areas were determined using the sum of the pixel intensities. **Panel B**: The fluorescent images were evaluated for maximum density of the green fluorescence pixels in the tumors. * = $P < 0.05$ vs. vehicle control and the error bars are SEMs.

bearing mice (normal SCID mouse serum calcium is approx. 10.5 mg/dl), but no significant changes were observed between the pamidronate treatment groups compared to the vehicle control treatment group (data not shown).

PTHrP, OPG, and IL-8 were expressed by the PC-3-GFP cells in vitro (220, 15, and 45 pg/μg cell protein/96 hr at 37°C, respectively) but sRANKL and IL-6 were undetectable. Non-tumor bearing, littermate control mice had undetectable serum PTHrP, OPG, IL-6, and sRANKL levels. The sera from the tumor bearing mice demonstrated PTHrP, OPG, and IL-8 expression, but sRANKL and IL-6 were not detectable. Serum OPG and PTHrP levels were significantly decreased in the high dose pamidronate treated group compared to the control group (76.5%, $P < 0.001$ and 33.3%, $P < 0.05$,

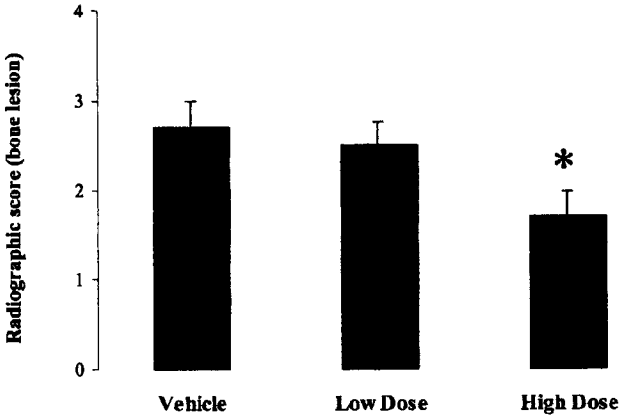

Fig. 3. Radiographic scoring of the mice tibiae demonstrated that pamidronate decreased the severity of the bone lesions. The radiographic images of the mouse tibiae injected with PC-3-GFP cells were evaluated by two observers and assigned a score. The semi-quantitation scoring method was formulated as 0 = no lesions, 1 = minor changes, 2 = small lesions, 3 = significant lesions (minor peripheral margin breaks, 1–10% of bone surface disrupted), 4 = significant lesions (major peripheral margin breaks. >10% of bone surface disrupted). * = $P < 0.05$ vs. vehicle control and the error bars are SEMs.

respectively). Figure 4 shows that the high-dose pamidronate-treated group also demonstrated a significant reduction in PTHrP compared to the control and low-dose groups, while in the low-dose pamidronate-treatment group PTHrP levels were reduced compared to the control group, but not significantly. Figure 5 shows the significant decrease in serum OPG expression with the high-dose pamidronate-treatment compared to the no treatment group. OPG and PTHrP were significantly correlated ($r = 0.486$, $P < 0.05$). There

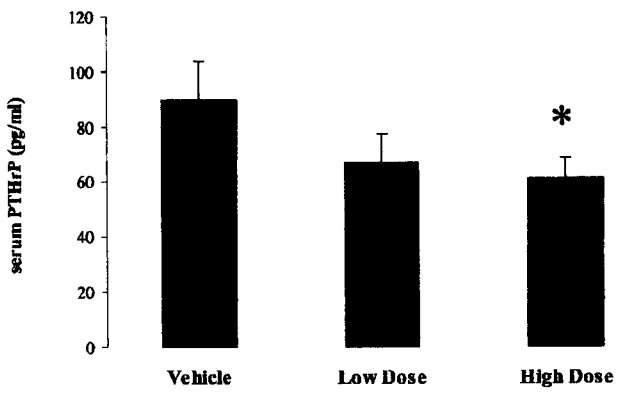

Fig. 4. Pamidronate treatment decreased serum PTHrP. The mice were bled 8 weeks after injection of PC-3-GFP cells and the PTHrP levels were measured in the sera. The asterisk indicates a significant difference compared to the control group based on a two-tailed Student t-test (* = $P < 0.05$) and the error bars are SEMs.

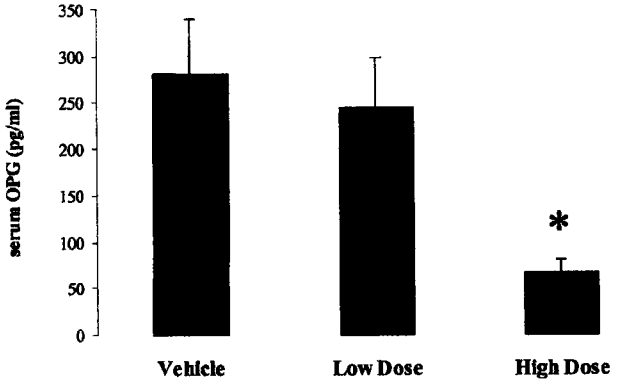

Fig. 5. Pamidronate treatment decreased serum OPG. The mice were bled 8 weeks after injection of PC-3-GFP cells and the OPG levels were measured in the sera. The asterisk indicates a significant difference compared to the control group based on a two-tailed Student t-test (* = $P < 0.05$) and the error bars are SEMs.

was no significant effect on IL-8 expression by pamidronate treatment compared to the control group (data not shown).

DISCUSSION

Our osseous-PCa model, consisting of direct injection of PCa cells into tibiae, is a useful tool for studying the effects of bisphosphonates on the skeletal progression of PCa. The model provides a reliable method for producing prostate carcinoma xenografts in bone, and tumor progression can be monitored by GFP imaging and X-ray. Pamidronate caused a dose-dependent reduction in bone involvement as assessed by severity of lesions on radiographs and by burden and density of the GPF-expressing tumor cells on fluorescent imaging.

The X-ray and GFP scores of the lesions gave similar scores and correlated with each other. The maximum green fluorescent pixel values, which were centered in the tumor cells growing in the bone rather than extraosseous tumor, were reduced in the high dose pamidronate treatment group compared to the control group, possibly reflecting a greater effect of bisphosphonates on tumor cells in the bone microenvironment. Once the tumor cells starting growing outside the bone, the pamidronate seemed to have little effect on its growth.

Lee et al. [30] demonstrated in culture studies that pamidronate had inhibitory effects on the growth of several PCa cell lines, including PC-3 cells, but only at the highest dose tested (100 μM). Other investigators have also found that bisphosphonates reduce growth of PCa bone metastases in animal models. Corey et al. [22] found that zolendronate, a third generation bisphosphonate, had inhibitory effects on the growth of PCa

osteoblastic and osteolytic bone metastases in their mouse model, but they did not observe any inhibitory effects on PCas growing outside of the bone milieu.

Our results suggest that PTHrP and OPG could be useful as biomarkers for bone metastasis in PCa. Serum levels of both proteins were elevated in animals carrying tibial metastases and levels were decreased by a treatment that reduced tumor burden. PTHrP is an oncoprotein that regulates the growth and proliferation of many common malignancies. Studies by our colleagues and us have demonstrated that prostatic PTHrP and OPG regulate tumor development, growth, and progression [8,9,31]. We demonstrated previously that PTHrP plays a role in the progression of PCa metastasis to the bone [8]. The decrease in PTHrP after pamidronate treatment could contribute to the efficacy of the therapy.

OPG produced by the PCa cells decreased with pamidronate therapy (Fig. 5). It is not clear what effect the reduction in OPG after pamidronate might have on the progression of skeletal metastases. On the one hand, decreased OPG could promote bone growth because OPG acts to inhibit osteoclastogensis by preventing RANKL binding to RANK. On the other hand, OPG is a survival factor in hormone-resistant PCa cells [32], so its loss could reduce the growth of the tumor cells. In either case, the decrease in PTHrP and OPG may reflect the reduction in bone tumor mass after therapy. Our results agree with clinical studies, where serum OPG levels significantly correlated with PCa progression and response to androgen therapy [33,34].

Bisphosphonates decrease osteoclast life span by promoting their apoptosis [18]. The bisphosphonate, pamidronate, has proven clinical efficacy for relieving bone pain associated with breast cancer metastases and has a promising outlook for PCa metastases [13–15]. Pamidronate is able to induce a decrease in bone resorption without significantly influencing bone formation [35]. Another bisphosphonate, zoledronic acid, appears to directly target PCa cells in addition to diminishing osteoclast activity at the metastatic site [14]. This provides a rationale for the use of bisphosphonates to treat bone pain and prevent skeletal complications. Further work in these areas will define the roles of bisphosphonates as agents with specific or direct anti-tumor activities. The roles of PTHrP and OPG as biomarkers to assess PCa tumor mass and monitor the effectiveness of bisphosphonate therapy warrant further studies.

ACKNOWLEDGMENTS

Expert technical help provided by C. Chalberg, K. Smith, S. Tu, V. Manheshwari, and J. Pache is greatly appreciated.

REFERENCES

1. Karayi MK, Markham AF. Molecular biology of prostate cancer. Prostate Cancer Prostatic Dis 2004;7(1):6–20.
2. Bubendorf L, Schopfer A, Wagner U, Sauter G, Moch H, Willi N, Gasser T C, Mihatsch MJ. Metastatic patterns of prostate cancer: An autopsy study of 1,589 patients. Hum Pathol 2000;31:578–583.
3. Wu G, Iwamura M, di Sant'Agnese PA, Deftos LJ, Cockett AT, Gershagen S. Characterization of the cell-specific expression of parathyroid hormone-related protein in normal and neoplastic prostate tissue. Urology 1998;51:110–120.
4. Brown JM, Corey E, Lee ZD, True LD, Yun TJ, Tondravi M, Vessella RL. Osteoprotegerin and rank ligand expression in prostate cancer. Urology 2001;57:611–616.
5. Ahmadpour OA, Burton DW, Tu S, Deftos LJ. Regulation of OPG/RANK/RANKL by PTHrP peptides in human prostate cancer cells. J Bone Miner Res 2002;17(1):S286.
6. Hofbauer LC, Khosla S, Dunstan CR, Lacey DL, Boyle WJ, Riggs BL. The roles of osteoprotegerin and osteoprotegerin ligand in the paracrine regulation of bone resorption. J Bone Miner Res 2000;15:2–12.
7. Walsh MC, Choi Y. Biology of the TRANCE axis. Cytokine Growth Factor Rev 2003;14:251–263.
8. Deftos LJ. Granin-A, parathyroid hormone-related protein, and calcitonin gene products in neuroendocrine prostate cancer. Prostate Suppl 1998;8:23–31.
9. Guise TA, Yin JJ, Taylor SD, Kumagai Y, Dallas M, Boyce BF, Yoneda T, Mundy GR. Evidence for a causal role of parathyroid hormone-related protein in the pathogenesis of human breast cancer-mediated osteolysis. J Clin Invest 1996;98:1544–1549.
10. Demers LM. Bone markers in the management of patients with skeletal metastases. Cancer 2003;97:874–879.
11. Deftos LJ. Prostate carcinoma: Production of bioactive factors. Cancer 2000;88:3002–3008.
12. Lee Y, Schwarz E, Davies M, Jo M, Gates J, Wu J, Zhang X, Lieberman JR. Differences in the cytokine profiles associated with prostate cancer cell induced osteoblastic and osteolytic lesions in bone. J Orthop Res 2003;21:62–72.
13. Ross JR, Saunders Y, Edmonds PM, Patel S, Wonderling D, Normand C, Broadley K. A systematic review of the role of bisphosphonates in metastatic disease. Health Technol Assess 2004;8(4):1–176.
14. Saad F, Gleason DM, Murray R, Tchekmedyian S, Venner P, Lacombe L, Chin JL, Vinholes JJ, Goas JA, Chen B. Zoledronic Acid Prostate Cancer Study Group. A randomized, placebo-controlled trial of zoledronic acid in patients with hormone-refractory metastatic prostate carcinoma. J Natl Cancer Inst 2002;94:1458–1468.
15. Body JJ, Mancini I. Bisphosphonates for cancer patients: Why, how, and when? Support Care Cancer 2002;10:399–407.
16. Zhang H, Yano S, Miki T, Goto H, Kanematsu T, Muguruma H, Uehara H, Sone S. A novel bisphosphonate minodronate (YM529) specifically inhibits osteolytic bone metastasis produced by human small-cell lung cancer cells in NK-cell depleted SCID mice. Clin Exp Metastasis 2003;20:153–159.
17. Conte PF, Latreille J, Mauriac L, Calabresi F, Santos R, Campos D, Bonneterre J, Francini G, Ford JM. Delay in progression of bone metastases in breast cancer patients treated with intravenous pamidronate: Results from a multinational randomized controlled trial. The Aredia Multinational Cooperative Group. J Clin Oncol 1996;14:2552–2559.

18. Hughes DE, Wright KR, Uy HL, Sasaki A, Yoneda T, Roodman GD, Mundy GR, Boyce BF. Bisphosphonates promote apoptosis in murine osteoclasts in vitro and in vivo. J Bone Miner Res 1995;10:1478–1487.
19. van der Pluijm G, Vloedgraven H, van Beek E, van der Wee Pals L, Lowik C, Papapoulos S. Bisphosphonates inhibit the adhesion of breast cancer cells to bone matrices in vitro. J Clin Invest 1996;98:698–705.
20. Fournier P, Boissier S, Filleur S, Guglielmi J, Cabon F, Colombel M, Clezardin P. Bisphosphonates inhibit angiogenesis in vitro and testosterone-stimulated vascular regrowth in the ventral prostate in castrated rats. Cancer Res 2002;62:6538–6544.
21. Lee MV, Fong EM, Singer FR, Guenette RS. Bisphosphonate treatment inhibits the growth of prostate cancer cells. Cancer Res 2001;61:2602–2608.
22. Corey E, Brown LG, Quinn JE, Poot M, Roudier MP, Higano CS, Vessella RL. Zoledronic acid exhibits inhibitory effects on osteoblastic and osteolytic metastases of prostate cancer. Clin Cancer Res 2003;9:295–306.
23. Kaighn M, Narayan K, Ohnuki Y, Lechner J, Jones L. Establishment and characterization of a human prostatic cell line (PC-3). Invest Urol 1979;17:16–23.
24. Maeda H, Hori S, Nishitoh H, Ichijo H, Ogawa O, Kakehi Y, Kakizuka A. Tumor growth inhibition by arsenic trioxide (As_2O_3) in the orthotopic metastasis model of androgen-independent prostate cancer. Cancer Res 2001;61:5432–5440.
25. Bastide C, Bagnis C, Mannoni P, Hassoun J, Bladou F. Nod Scid mouse model to study human prostate cancer. Prostate Cancer Prostatic Dis 2002;5:311–315.
26. Gujral A, Burton DW, Terkeltaub R, Deftos LJ. Parathyroid hormone-related protein induces interleukin 8 production by prostate cancer cells via a novel intracrine mechanism not mediated by its classical nuclear localization sequence. Cancer Res 2001;61:2282–2288.
27. van Bokhoven A, Varella-Garcia M, Korch C, Johannes WU, Smith EE, Miller HL, Nordeen SK, Miller GJ, Lucia MS. Molecular characterization of human prostate carcinoma cell lines. Prostate 2003;57:205–225.
28. Hoffman RM. Green fluorescent protein imaging of tumour growth, metastasis, and angiogenesis in mouse models. Lancet Oncology 2002;3:546–556.
29. Zar JH. Biostatistical analysis. Englewood Cliffs, NJ: Prentice-Hall; 1974.
30. Lee MV, Fong EM, Singer FR, Guenette RS. Bisphosphonate treatment inhibits the growth of prostate cancer cells. Cancer Res 2001;61:2602–2608.
31. Zhang J, Dai J, Qi Y, Lin DL, Smith P, Strayhorn C, Mizokami A, Fu Z, Westman J, Keller ET. Osteoprotegerin inhibits prostate cancer-induced osteoclastogenesis and prevents prostate tumor growth in the bone. J Clin Invest 2001;107:1235–1244.
32. Holen I, Croucher PI, Hamdy FC, Eaton CL. Osteoprotegerin (OPG) is a survival factor for human prostate cancer cells. Cancer Res 2002;621619–621623.
33. Brown JM, Vessella RL, Kostenuik PJ, Dunstan CR, Lange PH, Corey E. Serum osteoprotegerin levels are increased in patients with advanced prostate cancer. Clin Cancer Res 2001;7:2977–2983.
34. Eaton CL, Wells JM, Holen I, Croucher PI, Hamdy FC. Serum osteoprotegerin (OPG) levels are associated with disease progression and response to androgen ablation in patients with prostate cancer. Prostate 2004;59:304–310.
35. Reszka AA, Rodan GA. Bisphosphonate mechanism of action. Curr Rheumatol Rep 2003;5:65–74.